Displacement of alpha-actinin from the NMDA receptor NR1 C0 domain By Ca2+/calmodulin promotes CaMKII binding

ARTICLE *in* BIOCHEMISTRY · AUGUST 2007

Impact Factor: 3.02 · DOI: 10.1021/bi0623025 · Source: PubMed

8 AUTHORS, INCLUDING:

Zee A. Malik
University of California, Davis
16 PUBLICATIONS **260** CITATIONS
SEE PROFILE

Jason A Bartos
University of Minnesota Twin Cities
19 PUBLICATIONS **140** CITATIONS
SEE PROFILE

Published in final edited form as:
Biochemistry. 2007 July 24; 46(29): 8485–8497. doi:10.1021/bi0623025.

DISPLACEMENT OF α-ACTININ FROM THE NMDA RECEPTOR NR1 C0 DOMAIN BY Ca^{2+}/CALMODULIN PROMOTES CAMKII BINDING

Michelle A. Merrill[1], **Zulfiqar Malik**[1], **Zeynep Akyol**[2], **Jason A. Bartos**[1], **A. Soren Leonard**[1], **Andy Hudmon**[3,#], **Madeline A. Shea**[2], and **Johannes W. Hell**[*]

1*Department of Pharmacology, Roy J. and Lucille A. Carver College of Medicine, University of Iowa, Iowa City, IA 52242-1109, USA*

2*Department of Biochemistry, Roy J. and Lucille A. Carver College of Medicine, University of Iowa, Iowa City, IA 52242-1109, USA*

3*Department of Neurobiology, Stanford University, Stanford, CA 94305, USA*

Abstract

Ca^{2+} influx through the N-methyl-D-aspartate (NMDA)-type glutamate receptor triggers activation and postsynaptic accumulation of Ca^{2+}/calmodulin-dependent kinase II (CaMKII). CaMKII, calmodulin, and α-actinin directly bind to the short membrane proximal C0 domain of the C-terminal region of the NMDA receptor NR1 subunit. In a negative feedback loop, calmodulin mediates Ca^{2+}-dependent inactivation of the NMDA receptor by displacing α-actinin from NR1 C0 upon Ca^{2+} influx. We show that Ca^{2+}-depleted calmodulin and α-actinin simultaneously bind to NR1 C0. Upon addition of Ca^{2+}, calmodulin dislodges α-actinin. Either the N- or C-terminal half of calmodulin is sufficient for Ca^{2+}-induced displacement of α-actinin. While α-actinin directly antagonizes CaMKII binding to NR1 C0, the addition of Ca^{2+}/calmodulin shifts binding of NR1 C0 toward CaMKII by displacing α-actinin. Displacement of α-actinin results in the simultaneous binding of calmodulin and CaMKII to NR1 C0. Our results reveal an intricate mechanism whereby Ca^{2+} functions to govern the complex interactions between the two most prevalent signaling molecules in synaptic plasticity, the NMDA receptor and CaMKII.

N-methyl-D-aspartate (NMDA) receptors mediate Ca^{2+} influx at the postsynaptic site leading to the activation of Ca^{2+}/calmodulin-dependent kinase II (CaMKII) by Ca^{2+}/calmodulin (CaM) (1). CaMKII regulates various neuronal functions including ion-channel activity, neuronal excitability, and gene expression. Ca^{2+} influx through the NMDA receptor and subsequent activation of CaMKII are the key signaling steps in learning and memory and in longterm potentiation (LTP), which is thought to underlie memory formation (2–5). Activation of CaMKII by Ca^{2+}/CaM and the ensuing Thr^{286} autophosphorylation promotes CaMKII binding to several postsynaptic proteins including the NR1 (6,7), NR2A (8,9), and NR2B subunits (6,10–14) of the NMDA receptor (for review see (15,16)). CaMKII consists of 12 homologous subunits. Targeting stimulated CaMKII to the NMDA receptor would allow for fast and effective activation of additional subunits in the dodecameric CaMKII complex by NMDA receptor mediated Ca^{2+} influx. It also promotes specific and efficient phosphorylation of

Address correspondence to: Johannes W. Hell, Department of Pharmacology, Roy J. and Lucille A. Carver College of Medicine, University of Iowa, 51 Newton Road, 2-512 BSB, Iowa City, IA 52242-1109; Tel: (319) 384 4732; Fax: (319) 335 8930.
[#]Current Address: Department of Biochemistry and Molecular Biology, Indiana University, Indianapolis, IN, 46202

neighboring postsynaptic targets including α-amino-3-hydroxy-5-methyl-4-isoxazole propionic acid (AMPA)-type glutamate receptors (6,17–19).

The NMDA receptor is likely a tetramer consisting of two obligatory NR1 subunits and two NR2 (A–D) subunits (20–23). The cytosolic C-terminus of NR1 binds several postsynaptic proteins including CaM (24), α-actinin (25) and CaMKII (6,7). High affinity binding of CaMKII to NR1 requires autophosphorylation of Thr^{286} (7). Using peptide libraries of the C-terminal portion of NR1, we determined the amino acid sequence responsible for CaMKII, CaM and α-actinin binding to NR1 (7). All three proteins bind to residues 845–863 of the membrane-proximal C0 region (7), which likely adopts an α-helical conformation (26). Whereas the binding sequences for CaM and α-actinin overlap precisely, the CaMKII binding sequence is shifted by roughly one α-helical turn toward the N-terminus (7). These binding studies provide a molecular explanation for the competition of α-actinin with Ca^{2+}/CaM (7, 25) and with CaMKII (7) for binding to NR1 C0.

CaM is a highly conserved, 148 residue long ubiquitous Ca^{2+} sensor. The molecule is dumbbell shaped with the N- and C-domains separated by a flexible linker region. It consists of four EF-hand Ca^{2+}-binding motifs (I–IV). Sites I and II form the N-domain and sites III and IV the C-domain. CaM reduces NMDA receptor activity by displacing α-actinin from NR1 C0, thereby promoting desensitization (25,27–29). We recently showed that the C-but not N-domain binds to the NR1 C0 domain under Ca^{2+}-depleted (apo) conditions (26). This pre-association of apo-CaM with the NMDA receptor permits a quick and specific response upon NMDA receptor activation, as the ensuing Ca^{2+} influx triggers binding of the N-domain and re-arrangement of the C domain (26). The CaM-mediated negative feedback may be important under pathological conditions associated with an overabundance of Ca^{2+}, such as epilepsy or stroke.

Given the importance of CaMKII, CaM and α-actinin in NMDA receptor signaling under physiological and pathological conditions, it is essential to further our understanding of the precise molecular mechanisms regulating the interactions between these proteins. Here we address the critical questions of whether pre-associated apo-CaM and α-actinin simultaneously bind to NR1 C0 and how CaM affects CaMKII binding to NR1 C0 in the presence of α-actinin. We found that CaM does not compete with α-actinin for NR1 C0 binding under Ca^{2+}-depleted conditions. However, under Ca^{2+}-saturating conditions either the N- or C-terminal domain of CaM is sufficient to displace α-actinin, which in turn promotes CaMKII binding.

EXPERIMENTAL PROCEDURES

Materials

Amylose resin and anti-MBP antibodies were purchased from New England Biolabs, Inc. (Ispwich, MA), antibodies against anti-CaM from Zymed Laboratories, Inc. (San Francisco, CA), and ECL™, ECL-Plus™ and glutathione Sepharose from Amersham Pharmacia Biotech (Piscataway, NJ). The phosphospecific antibody recognizing CaMKII phosphorylated on T286 was purchased from Promega (Madison, WI). The CaMKII T305 phosphospecific antibody was kindly provided by Dr. Silva (University of California, Los Angeles)(30). Antibodies against CaMKIIα, α-actinin, and GST are as described in (7). Other reagents were obtained from established commercial suppliers and were of standard biochemical quality. Fluorescein-labeled NR1 C0 peptide (NR1C0p) covering residues 838–865 (fluorescein-SRHKDARRKQMQLAFAAVNVWRKNLQDR) was custom-made by the W.M. Keck Biotechnology Resource Center at Yale University (New Haven, CT) and purified by HPLC. A CaMKII peptide consisting of the CaM binding domain (CaMKIIp with amino acid sequence LKKFNARRKLKGAILTTMLA) was purchased from Calbiochem (La Jolla, CA). Recombinant rat calmodulin ($CaM_{1–148}$), N-terminal ($CaM_{1–80}$) and C-terminal ($CaM_{76–148}$) fragments were overexpressed in *Escherichia coli* as published (31). Ca^{2+} binding mutants of

full length CaM (E31Q/E67Q CaM and E104Q/E148Q Ca) were also expressed in *E. coli* as described (Evans & Shea, manuscript in preparation). These two mutants do not effectively bind Ca^{2+} in the N- and C-domain, respectively. Recombinant CaMKIIα was purified from *Spodoptera frugiperda* cells as detailed in (32) (Fig. 4) and (7) (Fig. 6).

Production of fusion proteins

The GST-tagged recombinant C-terminus of NR1 containing the C0 and C2′ segment (GST-NR1 C0-C2'), GST, and poly-His_6-tagged α-actinin-2 (encoding residues 344–894 of human α-actinin-2, contains also a T7 tag) were expressed in *E. coli* as given in (6,7). Human α-actinin-1 and -2 were subcloned into the pMAL-c2E vector (New England Biolabs, Ispwich, MA) placing the α-actinin ORFs in frame downstream of the *malE* coding sequence (encoding maltose binding protein, MBP). The templates used for the corresponding PCR reactions were pEGFP/α-actinin-1 (graciously provided by Dr. C. Otey, University of North Carolina, Chapel Hill, NC) (33,34), and pcDNA3/α-actinin-2 (kindly provided by Dr. M. Sheng, Massachusetts Institute of Technology, Boston, MA). Primers were designed such that an EcoRI site was integrated into the 5' primer and a SalI site into the 3' primer for both α-actinins. The sequences were 5'-GCT TGC CAT ATG GAA TTC ATG GAC CAT TAT GAT TCT CAG CAA ACC-3' and 5'-CCT TGC GTC GAC TTA GAG GTC ACT CTC GCC GTA CAG C-3' for α-actinin-1 and 5'-GCT TGC CAT ATG GAA TTC ATG AAC CAG ATA GAG CCC GGC-3' and 5'-CCT TGC GTC GAC CAT ATG CAG ATC GCT CTC CCC GTA GAG-3' for α-actinin-2. After PCR, the α-actinin products were cut with EcoRI and SalI and ligated into EcoRI-SalI digested pMAL-c2E. Positive clones were confirmed via sequencing before being expressed in *E. coli*.

α-Actinin and CaM binding and competition assays (Fig. 1–Fig. 3)

To examine α-actinin and CaM binding under Ca^{2+}-depleted conditions, glutathione Sepharose was incubated with 8 or 20 ng GST-NR1 C0-C2′ and washed. C0-C2′ is one of four different NR1 C-termini created by alternative splicing. It avoids the C1 exon, which encodes a second CaM binding site that is not relevant for binding of α-actinin or CaMKII to NR1 nor for CaM binding to the C0 region (7). CaM (1, 2.5 or 4 μM) and α-actinin (4 or 6 μM) were added in HEPES buffer (50 mM HEPES, 100 mM KCl, 5 mM NTA, 1mM MgCl, 50 μM EGTA; pH 7.4). NTA and EGTA are relatively weak and strong Ca^{2+} buffers, respectively. This Ca^{2+} buffer is typically used in our experiments when comparing Ca^{2+}-depleted with Ca^{2+}-saturated conditions (see next paragraph). In this experiment they eliminate traces of Ca^{2+} introduced as unavoidable minor contaminations of other reagents such as HEPES. We typically find total calcium in our buffers due to such contamination to be in the range of 1–5 μM as determined by atomic absorption spectrometry. The final incubation volume was 50 μl. The nominal final concentration of GST-NR1 C0-C2′ was either about 5 or 12.5 nM assuming that most fusion protein bound and remained on the resin during washing. Accordingly, CaM and α-actinin were in huge excess over GST-NR1 C0-C2′ so that their free concentration can be considered constant corresponding to the input. Samples were tilted at 4°C for 2 hours before two rapid washes (within less than 2.5 min as apo-CaM quickly dissociates from GST-NR1 C0-C2') with HEPES buffer containing 0.1% Triton X-100. Proteins were extracted using standard SDS sample buffer (7). EGTA (50 mM) was included in the sample buffer to chelate Ca^{2+}. Otherwise CaM migrates faster during SDS-PAGE when free Ca^{2+} present in the sample buffer as compared to conditions under which Ca^{2+} is chelated for reasons that are unclear (35,36). After SDS-PAGE, proteins were transferred onto polyvinylidene difluoride (PVDF) membranes. Membranes were probed with anti-CaM antibodies, stripped with SDS and dithiothreitol and reprobed with anti-GST to confirm comparable amounts of fusion protein were present in each sample.

To analyze the effect of Ca^{2+} on the competition of wild-type and mutant CaM on α-actinin binding to GST-NR1 C0-C2′ (Fig. 3), we used the above HEPES buffer containing 0.1% Triton X-100, which helps reducing non-specific binding of α-actinin. When indicated, 10 mM $CaCl_2$ was present in the sample so that Ca^{2+} is in excess of NTA and EGTA. The free Ca^{2+} concentration in this solution is 5.1 mM as calculated using published acid and ligand association constants for EGTA (37) and NTA (38). In these experiments α-actinin and CaM were added at final concentrations of 200 nM and 10 μM, respectively, to glutathione Sepharose preincubated as described above with 20 ng of GST-NR1 C0-C2′ fusion protein or equal amount of GST. Samples were tilted at 4°C for 2 hours before being washed with HEPES buffer containing 0.1% Triton X-100. Proteins were extracted, subjected to SDS-PAGE and transferred as above before being probed with anti-MBP.

CaMKII and CaM co-binding assays (Fig. 4)

Recombinant CaMKIIα (0.55 μg, 200 nM final nominal concentration if CaMKIIα would be in monomeric form) was incubated in 50 μl of 50 mM PIPES (pH 7.4), 1% BSA, 2 mM $MgCl_2$, 100 μM ATP, 1.5 mM $CaCl_2$, and 1 μM CaM to induce autophosphorylation. Incubations were performed for 1 minute on ice to ensure nearly exclusive autophosphorylation of Thr^{286} and to suppress phosphorylation of other sites (see Ref. (39,40) and Fig. 4A). For control experiments with unphosphorylated CaMKII, ATP was omitted. After the brief phosphorylation reaction, kinase activity was inhibited by chelating Mg^{2+} with 10 mM EDTA, which was added together with 500 mM NaCl and 0.1% Tween (final concentrations; NaCl and Tween help reduce nonspecific interactions). In parallel, 20 ng of GST-NR1 C0-C2′ fusion protein or GST (nominal concentration in 50 μl would be 11 nM) were incubated with glutathione Sepharose and washed three times. These resins were then incubated with the pretreated CaMKII at 4° C for two hours before washing three times with TBS (10 mM Tris-HCl, pH 7.4, 150 mM NaCl) containing 0.1% Triton X-100, with 10 min in between washing steps to allow unbinding of non-specifically bound CaMKII from the resin. The CaMKII/NR1 C0-C2′ fusion protein complex was incubated with increasing amounts of CaM in 25 mM PIPES, 150 mM NaCl, 10 mM $CaCl_2$ and 0.1% Triton X-100 at 4° C for four hours and washed as before except without extended time periods between washing steps to prevent extensive unbinding of CaM during washing. Proteins were extracted, subjected to SDS-PAGE and transferred to PVDF as described above. Membranes were stained with Ponceau S to verify that equal amounts of the GST fusion proteins were present before being cut to probe the upper portion with an anti-CaMKII antibody and the lower portion with a mouse monoclonal anti-CaM antibody (Zymed Laboratories, Inc., San Francisco, CA).

α-Actinin, CaM and CaMKII co-binding assays (Fig. 6)

GST-NR1 C0-C2′ (160 ng; nominal concentration is about 90 nM in the 50 μl incubation volume assuming most fusion protein was retained by the resin) or GST alone (160 ng) was immobilized on glutathione Sepharose, washed, and incubated with 1 μM His_6-tagged α-actinin-2 (residues 344–894, also containing a T7 tag) in 50 μl 150 mM NaCl, 50 mM HEPES-NaOH, pH 7.4, for 2 hours under tilting at 4° C. In parallel, recombinant CaMKIIα (1.1 μg) was preincubated for 1 minute on ice (to promote Thr^{286} autophosphorylation) in 50 μl 50 mM HEPES-NaOH, pH 7.4, 10 mM $MgCl_2$, 500 μM $CaCl_2$, 0.2 μM CaM, and 500 μM ATP before addition to the glutathione Sepharose-GST-NR1 C0-C2′/α-actinin-2 mixture (final concentration of CaMKII and CaM was 0.1 μM in the final volume of 100 μl). Additional CaM was added to samples for a final concentration of 1.0 and 10 μM in parallel samples. Samples were tilted at 4°C for another 2 hours, washed with TBS containing 0.1% Triton X-100, and analyzed by immunoblotting with anti-CaMKII, and, after stripping, anti-T7 (Invitrogen Corporation, Carlsbad, CA).

For quantification of immunoblot signals, multiple exposures with increasing time were performed to ensure that chemiluminescent film signals were in the linear range. Basically, doubling of the exposure time has to lead to a doubling of the signal as we published earlier (41,42). Signals were scanned using an Epson Perfection 4180 Photo flatbed scanner and EPSONscan software (42). To ensure that signals were comparable between different films and not distorted by using non-linear contrast functions, neither autocontrast nor any other manipulations of contrast such as non-linear transformation were applied throughout the whole procedure. Adobe Photoshop sets the whitest pixel equal to 255 and the darkest signal to 0. To measure increases in original film signals, which are dark, as increases in pixel values, images were inverted. Individual bands were quantified for mean intensity by drawing equal sized boxes around each band and using the histogram function of Adobe Photoshop to calculate mean intensity. A same size box was used to subtract background from a nearby area on the film. Background generally consisted of no more than 5–10% of the total signal. Signals were compared using a paired-t-test and significance was established if $p > 0.05$.

Fluorescence emission spectra scans (Fig. 5A–D)

Competition between CaMKIIp and NR1C0p for binding to Ca^{2+}-saturated CaM was studied by equilibrating full length CaM ($CaM_{1–148}$) or its individual domain fragments ($CaM_{1–80}$ and $CaM_{76–148}$) with NR1C0p at a 1:1 ratio and adding successive aliquots of CaMKIIp reaching a final CaMKIIp:NR1C0p ratio of 2.29 for full length CaM and 4.58 for individual domain fragments under Ca^{2+}-saturated conditions. Fluorescence emission spectra were collected before and after equilibration with NR1C0p and after each addition of CaMKIIp using an SLM-4800 spectrofluorimeter (SLM Urbana, IL). Emission spectra of NR1C0p (2.54 μM) were monitored using fluorescence of the tryptophan in NR1C0p (λ_{ex} of 297 nm) with 4 nm slits for full length CaM (2.54 μM) and 8 nm slits for CaM domain fragments (2.37 μM). Emission spectra of Ca^{2+}-saturated CaM under identical conditions were subtracted from spectra of peptide/CaM mixtures to account for the small contribution from Tyr 99 and Tyr 138 in CaM (CaM does not contain a tryptophan). All spectra within one titration were normalized relative to the maximum intensity of NR1C0p at 350 nm. The buffer conditions were 50 mM HEPES, 100 mM KCl, 0.5 mM EGTA, 0.5 mM NTA, 5 mM $CaCl_2$, pH 7.4, at 22 °C.

Fluorescence anisotropy (Fig. 1D, E and Fig. 5 E)

Fluorescence anisotropy was measured using a Fluorolog-3 (Horiba Jobin Yvon, NJ) spectrofluorimeter using the same experimental conditions as those used for spectra described above. The wavelengths were λ_{ex} of 496 nm and λ_{em} of 520 nm with 200 nM NR1C0p when utilizing the fluorescein tag on the NR1C0p and λ_{ex} of 297 nm and λ_{em} of 350 nm when utilizing tryptophan in NR1C0p (CaM does not contain tryptophan). For titration of NR1C0p with α-actinin-1 and -2 fluorescein fluorescence anisotropy was determined for NR1C0p (10 nM) alone and with increasing α-actinin concentrations. For displacement of CaM from NR1C0p by CaMKIIp as monitored by tryptophan fluorescence anisotropy, 4.17 μM NR1C0p and 3.9 μM $CaM_{1–148}$ (i.e., a slight excess of NR1C0p) were titrated with increasing concentrations of CaMKIIp. Fluorescence anisotropy was calculated using the standard equation: $R=(I_{VV}-GI_{VH})/(I_{VV}+2GI_{VH})$(43).

Fluorescence polarization (Fig. 5F)

Fluorescence polarization studies were performed under the same buffer conditions described for emission spectra and anisotropy using a Victor plate reader (PerkinElmer, MA) to monitor the change in the fluorescein moiety (λ_{ex} of 495 nm and λ_{em} of 518 nm) attached to NR1C0p. Concentration of NR1C0p was 0.91 μM and of $CaM_{1–148}$ 0.638 μM.

Protein concentrations were determined with standard Bradford (BioRad) and bicinchoninic acid (Pierce) microtiter plate assays following the instructions of the manufacturers using bovine serum albumin as a standard.

RESULTS

We have previously shown that α-actinin, CaM, and CaMKII, bind to an overlapping region within the NR1 C0 region (7). CaM and α-actinin compete with each other for binding to NR1 C0 in the presence of Ca^{2+} (7,25). However, apo-CaM can pre-associate with NR1 C0 under Ca^{2+}-depleted conditions (26). This association is thought to be crucial for fast and specific regulation of NMDA receptor activity by a negative feedback mechanism (26). Accordingly, Ca^{2+} influx leads to displacement of NR1-associated α-actinin by CaM, thereby triggering desensitization of the NMDA receptor (28,29). If this model is correct apo-CaM and α-actinin must be able to bind simultaneously to NR1 C0. To test this model we first determined the binding affinity for α-actinin before analyzing the hypothesized simultaneous binding of apo-CaM and α-actinin with NR1 C0.

Affinity of GST-NR1 C0-C2′ is higher for α-actinin-1 than α-actinin-2

The α-actinin family is comprised of 4 genes that encode the homologous α-actinin-1, -2, -3, and -4 isoforms. The C-terminal regions contain two EF-hand motifs, which seem to be functional with respect to Ca^{2+} binding for α-actinin-1 and -4 but not -2 and -3 (44,45). α-Actinin-2 was originally identified as the NR1 C0 binding partner (25,28). Physiological evaluations of this interaction, therefore, focused on α-actinin-2 and did not specifically test effects by α-actinin-1 (28,29). However, two different proteomic analyses of highly purified postsynaptic density fractions suggest that α-actinin-1 is more abundant than α-actinin-2 (46, 47). We observed that α-actinin-1 binding to NR1 C0-C2′ is much stronger than binding of α-actinin-2. Using immobilized GST-NR1 C0-C2′ for pull down experiments with recombinant, purified MBP-tagged α-actinin-1 and -2, we consistently found more α-actinin-1 than -2 in the precipitates (Fig. 1A, lanes 1,2) even though equal amounts of both α-actinins were present in each sample during binding (Fig. 1A, lanes 7,8). We also tested whether Ca^{2+} itself would influence α-actinin binding to NR1 C0 as α-actinin-1 has a pair of functional EF hands at its C-terminus. However, addition of Ca^{2+} affected neither α-actinin-1 nor -2 binding in this assay (Fig. 1A, compare lanes 1 and 2 with 3 and 4; see also below).

GST-NR1 C0-C2′ was incubated with increasing amounts of MBP-α-actinin-1 and -2 to determine the apparent Kd values for these interactions in the pull-down experiments. α-Actinin-1 resulted in a clear saturation curve indicating an apparent Kd value of ~87 nM (Fig. 1B,C). α-Actinin-2 binding was too weak to come reasonably close to saturation in these pull-down assays. Therefore, we resorted to titrating α-actinin-2 against the synthetic NR1C0p peptide that covers the whole C0 segment and carries a fluorescein label at its N-terminus using fluorescence anisotropy as a read out (26). This method does not require a washing step, which would preserve the weaker α-actinin-2 binding. These experiments resulted in a saturation curve with a Kd value of 2.75 μM (Fig. 1D). Ca^{2+} did not alter the affinity in these experiments (Fig. 1D).

We used the same fluorescence anisotropy assay to further evaluate whether Ca^{2+} might regulate α-actinin-1 binding to NR1 C0. The Kd in the presence and absence of Ca^{2+} was 237 and 239 nM, respectively (Fig. 1E). These values are higher than for the Kd obtained in the pull down experiments (Fig. 1 B, C) likely because the synthetic peptide has a higher propensity to be unfolded compared to the fusion protein, thereby shifting the binding equilibrium towards the unbound peptide.

α-Actinin and apo-CaM interact simultaneously with GST-NR1 C0-C2′ under Ca^{2+}-depleted conditions

Although α-actinin competes with Ca^{2+}-CaM for binding to NR1 C0 (25,29), we tested whether apo-CaM can pre-associate with the α-actinin-NR1 C0 complex. We used a small amount of NR1 C0-C2′ (8–20 ng corresponding to about 5–12.5 nM nominal concentration in the 50 μl incubation volume) to ensure saturation with α-actinin-1, which was added at a final concentration of 6 μM, in great excess of its apparent Kd value for binding to GST-NR1 C0-C2’ (87 nM; see Fig. 1). Apo-CaM was added at a final concentration of 2.5 μM. We determined earlier that the Kd of apo-CaM for NR1 C0 is 2.25 μM (26). For that reason, a concentration of apo-CaM in this range is optimal for detection of a potential competition by α-actinin. Addition of α-actinin-1 never reduced apo-CaM binding to GST-NR1 C0-C2’ in multiple independent experiments (Fig. 2A, B). To the contrary, CaM binding to GST-NR1 C0-C2′ was increased in the presence of α-actinin. To exclude the possibility that α-actinin and CaM bind directly, we preformed in vitro binding assays immobilizing MBP-tagged α-actinin-1 or -2 or MBP alone and added 50 μM CaM in the presence and absence of Ca^{2+}. No interaction of apo-CaM or Ca^{2+}-CaM with α-actinin was detectable (Fig. 2C). Accordingly, under the conditions of these experiments CaM does not directly bind to α-actinin. Hence, apo-CaM binding to the GST-NR1 C0-C2’ - α-actinin-1 complex (Fig. 2A) is through binding to NR1 C0 and not to α-actinin-1. Because pull-down of apo-CaM by GST-NR1 C0-C2′ is not reduced in the presence of a saturating amount of α-actinin-1, i.e., when α-actinin-1 occupies nearly all NR1-C0 sites, we conclude that apo-CaM and α-actinin can simultaneously bind to NR1 C0. The most likely explanation for the increase in CaM binding to NR1 C0 in the presence of α-actinin is that binding of either CaM or α-actinin produces a change in the structure of NR1 C0 that promotes the association with the other binding partner. Our earlier studies monitoring circular dichroism have shown that a synthetic NR1 C0 peptide is unstructured in solution when none of its interaction partners is present (26). Combining this peptide with either apo-CaM or Ca^{2+}-CaM, which itself has several α-helices, increases the α-helical content in the solution likely because CaM binding to the NR1 C0 peptide induces an α-helical conformation of the peptide (26). Similarly, α-actinin might promote an α-helical structure in the C0 domain of the GST-NR1 C0-C2′ fusion protein, thereby promoting association of apo-CaM. The alternative explanation that binding of α-actinin-1 to GST-NR1 C0-C2’ creates a CaM binding site on α-actinin-1 that is not detectable in the absence of NR1 C0 binding is unlikely because Ca^{2+}-CaM actually displace α-actinin-1 from the GST-NR1 C0-C2’ complex (see Fig. 3).

Isolated N- and C-domain of CaM displaces α-actinin from GST-NR1 C0-C2′ with Ca^{2+} present

Our earlier data indicate that under apo conditions, CaM binds with its C- but not N-domain to NR1 C0. Upon addition of Ca^{2+}, the NR1C0p - C-domain complex undergoes a conformational change and the otherwise extended N-domain collapses onto C0 in the complex between NR1C0p and full length CaM (26). To investigate whether the N- or the C-domain of CaM dislodges α-actinin from GST-NR1 C0-C2’ upon addition of Ca^{2+}, we used recombinant purified full-length $CaM_{1–148}$, $CaM_{1–80}$ (the N-terminal domain followed by the linker region), and $CaM_{76–180}$ (linker region followed by the C-terminal domain) for in vitro binding assays under Ca^{2+}-depleted and Ca^{2+}-saturated conditions. As expected, full-length wild-type $CaM_{1–148}$ competed with α-actinin in the presence but not absence of Ca^{2+} (Fig. 3). In addition, either the N-terminal ($CaM_{1–80}$) or C-terminal region ($CaM_{76–180}$) was sufficient to displace α-actinin from NR1 C0 upon addition of Ca^{2+}. To further test the ability of both the N- and C-domain to displace α-actinin, we used two full-length CaM mutants that do not bind Ca^{2+} in either the N- or C-domain (E31Q/E67Q CaM and E104Q/E148Q CaM, respectively). In agreement with the findings with isolated N- and C-domain, both E31Q/E67Q CaM and E104Q/E148Q CaM were able to displace α-actinin from NR1 C0 (Fig. 3). Accordingly, CaM does not need to be tethered via its C domain in order for the N domain to displace α-actinin upon the binding of Ca^{2+}. However, this observation does not exclude that pre-association of

apo-CaM with NR1 C0 via its C-domain leads to more effective displacement of α-actinin from NR1 C0 as compared to non-associated CaM. Addition of Ca^{2+} a complex between the C domain of CaM with the N domain lacking induces a conformational change of this complex (26). Our findings that addition of Ca^{2+} with the C domain alone or with E31Q/E67Q CaM leads to displace of α-actinin from GST-NR1 C0-C2' thus indicate that those conformational changes are sufficient for displace of α-actinin. Taken together these data strongly support the idea that either of the N- or C-terminal domains of CaM is sufficient to displace α-actinin in the presence of Ca^{2+}. The addition of Ca^{2+} in the absence of CaM in these binding conditions did not change α-actinin binding to NR1 C0-C2′ (see also Fig. 1), excluding side effects of Ca^{2+}. Accordingly, the Ca^{2+}-induced effects observed in the presence of the CaM polypeptides are specifically mediated by CaM.

CaMKII and Ca^{2+}-CaM simultaneously bind to the NR1 C0 region

Ca^{2+} influx through the NMDA receptor stimulates CaMKII binding to the receptor with NR1 C0 being one of the three high affinity attachment sites for CaMKII (6,7). However, Ca^{2+}-CaM effectively competes with α-actinin for binding to this very site (Fig. 3; (7,25)). If the same competition were to occur between Ca^{2+}-CaM and CaMKII, Ca^{2+} influx would diminish rather than promote CaMKII binding to NR1 C0 in intact neurons. Therefore, we determined whether Ca^{2+}-CaM displaces CaMKII from NR1 C0 or permits concurrent binding of CaMKII. Upon binding Ca^{2+}-CaM, CaMKII can phosphorylate itself on T286 affording it prolonged kinase activity following the removal of Ca^{2+}-CaM. Upon more prolonged incubation CaMKII autophosphorylates itself on T305/306, which prevents future binding of CaM until dephosphorylation. Because this phosphorylation reduces to some degree CaMKII binding to NR1C0 (7), we incubated CaMKII for only 30 sec with Ca^{2+}-CaM and Mg-ATP on ice to specifically induce autophosphorylation of T286 and not T305/306; the autophosphorylation reaction was terminated with EDTA to chelate Mg^{2+}. Fig. 4 illustrates that this brief incubation in the presence of Ca^{2+}-CaM and Mg-ATP led to phosphorylation of T286 but not T305/306 (middle lane). As negative control, incubating CaMKII with Ca^{2+}-CaM but not ATP produced no autophosphorylation (left lane). Accordingly, the phosphospecific antibodies used in the immunoblots only recognized the respective sites when autophosphorylated, as expected. As positive control for the T305/306-directed phosphospecific antibody, CaMKII was incubated with CaM on ice for 30 seconds, EGTA was added to the mixture, and the kinase was incubated at 30°C for an additional 10 minutes. This procedure causes "hyperphosphorylation" of CaMKII, which is characterized by a slight upward shift of the corresponding band during SDS-PAGE, which in turn is correlated with phosphorylation of T305 and T306 on top of T286 phosphorylation (right lane).

To examine the effect of increasing CaM concentration on CaMKII binding, an aliquot of Thr^{286} phosphorylated CaMKII was added to GST-NR1 C0-C2′ or GST, which had been immobilized on glutathione Sepharose; samples were washed prior to the addition of CaM. This approach using pre-binding of CaMKII to immobilized GST-NR1 C0-C2′ allows removal of unbound Ca^{2+}-CaM along with ATP and free CaMKII. As previously shown (7,12), CaMKII must be autophosphorylated on Thr^{286} for binding to NR1 C0 (Fig. 4A, compare lane 1 with lanes 2 and 3). Extensive incubation of the resin-adsorbed GST-NR1 C0-C2′-CaMKII complexes with increasing concentrations of Ca^{2+}-CaM (up to 50 μM) did not change the amount of CaMKII binding to GST-NR1 C0-C2′ GST fusion protein (Fig. 4B). Immunosignals for CaMKII and CaM were quantified for samples without CaM versus 50 μM CaM in these experiments after digitalization by determining the mean density with Adobe Photoshop. There was no statistical difference in the immunosignal of CaMKII in the absence or presence of 50 μM CaM, as tested by a paired Student's t-test (Fig. 4C).

Ca^{2+}-CaM binding to the GST-NR1 C0-C2′ / CaMKII complex was near or at saturation at 50 μM (Fig. 4D). The relatively high apparent Kd (low μM) for Ca^{2+}-CaM binding in these experiments is due to washing of the samples resulting in an inevitable loss of some CaM (24,26). Nevertheless, our data show that 50 μM Ca^{2+}-CaM saturates NR1 C0 in these experiments, i.e., it occupies nearly all CaM binding sites (NR1 C0 and CaMKII). We would expect a reduction in the final CaMKII pull-down if Ca^{2+}-CaM displaced CaMKII, as it does with α-actinin (Fig. 3). The lack of such a reduction in CaMKII binding indicates that CaMKII and Ca^{2+}-CaM can simultaneously bind to NR1 C0.

Competition between NR1C0p and CaMKIIp for CaM binding

CaMKII itself strongly binds Ca^{2+}-CaM, especially when Thr^{286} is autophosphorylated. Previous studies indicate that binding of Ca^{2+}-CaM to CaMKII requires both, the N- and C-domain of CaM (48). Furthermore, Ca^{2+}-CaM binding to NR1 C0 involves both CaM domains (26). Nevertheless, we evaluated the possibility that a single CaM molecule might simultaneously bind NR1 C0 and CaMKII, acting as a bridge between CaMKII and NR1 C0. The NR1 C0-derived peptide NR1C0p has a single tryptophan residue (Trp^{21}) with an emission λ_{max} of 350 nm in the absence of CaM. Under Ca^{2+}-saturating conditions, the emission λ_{max} shifted to a lower wavelength (331 nm) upon binding either full-length CaM or its individual N- or C-domain fragments (Fig. 5 A–C; compare black lines in the absence of CaM with red lines in the presence of CaM) (26). This shift indicates that a complex is formed between CaM and the NR1C0p peptide with Trp^{21} of the peptide buried in a more hydrophobic environment upon CaM binding. The effect of the peptide CaMKIIp, which is derived from the CaM binding site on CaMKII, was evaluated in these spectroscopic assays. Addition of up to 4.58 eq of the CaMKIIp to either NR1C0p-$CaM_{1–80}$ (Fig. 5A) or NR1C0p-$CaM_{76–148}$ complexes (Fig. 5B) produced only minimal changes in λ_{max}. In contrast, addition of 2.29 eq CaMKIIp to NR1C0p-$CaM_{1–148}$ (Fig. 5C) caused the λ_{max} to shift from 331 nm (i.e., buried) back to 350 nm (i.e., free peptide, with the Trp exposed to buffer; red dotted line). Accordingly, the equilibrium of the NR1C0p-$CaM_{1–148}$ complex formation was shifted back so that virtually all NR1C0p was released from its complex with $CaM_{1–148}$ as virtually all $CaM_{1–148}$ present in the solution associated with the CaMKIIp. In other words, by effectively competing with NR1C0p for binding to $CaM_{1–148}$ CaMKIIp displaced NR1C0p from $CaM_{1–148}$. We conclude that NR1C0p and CaMKIIp cannot simultaneously associate with $CaM_{1–148}$. Otherwise, addition of CaMKIIp would lead to no or perhaps a partial rather than full reversal of the left-shift in the Trp^{21} fluorescence induced by the initial addition of $CaM_{1–148}$. The addition of CaMKIIp caused a decrease in intensity and shift in peak intensity at a CaMKIIp:NR1C0p ratio of 0.92 (Fig. 5C) suggesting that both peptides have similar affinities for Ca^{2+}-saturated $CaM_{1–148}$. Figure 5D shows the decrease in the fluorescence intensity at 331 nm due to disruption of the NR1C0p-$CaM_{1–148}$ complex. The position and intensity of the final emission spectrum demonstrated that virtually all of the NR1C0p was displaced from $CaM_{1–148}$ by addition of excess CaMKIIp. Accordingly, as the concentration of CaMKIIp increases, an increasing amount of CaM is redistributed from NR1C0p to CaMKIIp.

Competition between NR1C0p and CaMKIIP for CaM binding was also examined using fluorescence anisotropy to monitor the tryptophan signal of NR1C0p (Fig. 5E) and using fluorescence polarization to monitor the change in the fluorescein moiety attached to the N-terminus of NR1C0p (Fig. 5F). Both measures are a reflection of the tumbling rate of a fluorescent molecule. The larger a molecular complex is the slower its tumbling motion and the higher the degree to which polarization of the exciting light is preserved when emitted. An increase in fluorescence anisotropy or polarization for NR1C0p upon addition of CaM indicates binding of CaM and a decrease upon subsequent addition of the CaMKIIp displacement of CaM from NR1C0p. NR1C0p under Ca^{2+}-saturated conditions had an intrinsic anisotropy of 0.055 and the NR1C0p-$CaM_{1–148}$ complex had an anisotropy value of 0.0878. CaMKIIp began

displacing NR1C0p at CaMKIIp:NR1C0p ratio of 1.03, consistent with the emission studies. A quasi complete displacement was achieved by a ratio of 2.05, which freed the NR1C0p causing it to tumble with an anisotropy of ~0.056 (Fig. 5E). Control experiments showed that CaMKIIp cannot displace NR1C0p under apo conditions and that there is no interaction between CaMKIIp and NR1C0p (data not shown). Analogous results were obtained when measuring fluorescence polarization of the fluorescein tag (Fig. 5F). These results indicate that CaM and NR1C0p cannot readily form a trimeric complex with CaMKIIp. They argue against a model in which Ca^{2+}-CaM would simultaneously bind to NR1 C0 and CaMKII, thereby acting as an adaptor between them. Rather our results suggest that binding of CaMKII to NR1 C0 is direct, likely involving a region on CaMKII other than its own CaM binding site.

Ca^{2+}-CaM promotes CaMKII binding to NR1 C0 by displacing α-actinin

Earlier studies have shown that CaMKII competes with α-actinin-2 for NR1 C0 binding with a half-maximal inhibition occurring at ~1 μM α-actinin (7). Given that Ca^{2+}-CaM directly antagonizes the binding of α-actinin (7,25) but not of CaMKII (Fig. 4) to NR1 C0, we hypothesized that in the absence of Ca^{2+}, apo-CaM and α-actinin simultaneously associate with NR1 C0 allowing α-actinin to effectively compete with CaMKII for C0 binding. Upon addition of Ca^{2+}, so our hypothesis, Ca^{2+}-CaM dislodges α-actinin, thereby promoting CaMKII binding to NR1 C0 (Fig. 6A). To test this hypothesis, we immobilized GST-NR1 C0-C2′ on glutathione Sepharose (100 nM nominal concentration in the 50 μl incubation volume), washed, and pre-bound 1 μM α-actinin. Without washing, we then added 0.1 μM CaMKII pretreated to induce autophosphorylation of Thr^{286}. Similar to previous studies (7), α-actinin out competes CaMKII for binding to GST-NR1 C0-C2′ in the presence of low concentration of Ca^{2+}-CaM (0.1 μM presumably just enough to bind and activate the 0.1 μM CaMKII; Fig 6B). However, raising the Ca^{2+}-CaM concentration to 1 and 10 μM (the latter should saturate GST-NR1 C0-C2′ with Ca^{2+}-CaM) increasingly attenuated α-actinin binding and concomitantly elevated CaMKII binding to GST-NR1 C0-C2′. Accordingly, in the presence of Ca^{2+}, CaM shifts the binding toward CaMKII by competing with α-actinin.

DISCUSSION

NMDA receptor-mediated Ca^{2+} influx and the ensuing activation of CaMKII are central events in LTP and memory formation (2–5). LTP is largely restricted to those synapses that experience an activity pattern suitable for induction of LTP. For these reasons recruitment of CaMKII upon Ca^{2+} influx through the NMDA receptor to postsynaptic sites has received widespread attention (e.g., Refs. (6,13,14,49–54)). CaMKII binding to several postsynaptic interaction partners is activity-driven, i.e., the binding requires activation of CaMKII by Ca^{2+}/CaM. The two most prominent strictly activity-driven CaMKII attachment sites at the postsynaptic site are the C-termini of NR1 and NR2B (15,16). CaMKII binding to NR1-C0 depends on Ca^{2+}/CaM-induced autophosphorylation of CaMKII (6,7). NR2B binding requires either Ca^{2+}/CaM binding to CaMKII or CaMKII autophosphorylation (6,7,10–12). Some of the other postsynaptic interaction partners also show activity-driven CaMKII binding but in these cases this requirement is not absolute (e.g., densin-180 (55,56)) or the affinity of the interaction appears to be substantially less than for NR1 or NR2B binding (e.g., NR2A (6,8,10,11)) (see Refs. (15,16) for more detailed discussions). Here we focus on the interplay of NR1 with CaM, CaMKII, and α-actinin.

We showed earlier that α-actinin competes with CaMKII for binding to NR1 C0 (7). Given that Ca^{2+}/CaM dislodges α-actinin (7,25), we hypothesized that displacement of α-actinin by Ca^{2+}/CaM would promote CaMKII binding upon Ca^{2+} influx. Otherwise, Ca^{2+} influx and CaM association with NR1 C0 would occlude CaMKII binding rather than promote postsynaptic recruitment of CaMKII. Indeed, we show that CaMKII binding is not affected by saturated

binding of CaM to NR1 C0 indicating that Ca^{2+}/CaM and CaMKII simultaneously bind to NR1 C0.

Given that CaM binds both NR1 C0 and CaMKII, it was conceivable that CaM acts as a bridge between these two proteins with its N-domain interacting with one and the C-domain with the other binding partner. Using a peptide spanning most of the NR1 C0 domain (NR1 C0p) and a peptide covering the CaM binding domain of CaMKII (CaMKIIp) we investigated whether CaM could simultaneously bind to both peptides. Binding of full-length CaM to the peptides was competitive and exclusive, indicating that CaM cannot bind concomitantly to both NR1 C0 and CaMKII. These data are not surprising given that x-ray crystallography has shown that both domains of CaM are involved in CaMKII binding (48). Furthermore, our results show that CaMKIIp could not displace the NR1C0p from either the N- or the C-domain of CaM. The simplest explanation is that in contrast to the NR1 C0p, the CaMKIIp requires full length CaM for high affinity binding.

How do CaM and CaMKII simultaneously bind to NR1 C0? In the absence of crystallographic or NMR structural data we cannot answer this question. However, our previous peptide studies indicate that optimal binding regions in NR1 C0 for CaMKII and CaM are shifted by about 4 residues so that they only partially overlap (7). Similar more recent peptide studies in which certain residues in NR1 C0 were replaced by glutamate indicate that different sides of the predicted NR1 C0 α-helix are critical for CaM versus CaMKII binding (Leonard, Shea, and Hell, unpublished). We thus propose that CaM and CaMKII basically bind in a staggered formation to different sides of the putative NR1 C0 α-helix. This arrangement might allow simultaneous binding of CaM and CaMKII, whereas the presence of α-actinin, which is larger than CaM, would hinder access of CaMKII to its precise binding site on NR1 C0.

To test our model, we examined the effect of increasing amounts of Ca^{2+}/CaM on binding of CaMKII and α-actinin to GST-NR1 C0-C2', with the latter three being present in constant amounts. As we showed previously (7), with low amounts of total CaM present, which is largely bound to the equimolar CaMKII under our conditions, α-actinin effectively competed with CaMKII for association with GST-NR1 C0-C2'. However, increasing the CaM concentration attenuated α-actinin binding and concomitantly elevated CaMKII binding to GST-NR1 C0-C2' demonstrating that CaMKII can simultaneously bind with CaM to NR1 C0. We propose that at the postsynaptic membrane under resting conditions apo-CaM is preassociated via its C-domain with the NR1 C0 region. ApoCaM permits simultaneous α-actinin binding to NR1 C0, which prevents CaMKII from associating with NR1 C0. Upon Ca^{2+} influx, CaM displaces α-actinin allowing for CaMKII binding to NR1 C0.

CaMKII can also directly bind to α-actinin-2 (Leonard and Hell, unpublished data) (14,56, 57). However, this interaction is blocked in the presence of Ca^{2+}/CaM (13) or by autophosphorylation of threonine 305 and 306 in the CaM binding region of CaMKII (13). Thus, it appears that CaMKII binding to α-actinin-2 depends on the availability and conformation of the CaM binding region of CaMKII. In our α-actinin, CaM, CaMKII co-binding assays (Fig. 6B), the lowest concentration of Ca^{2+}/CaM present was equimolar to the concentration of CaMKII. At this concentration Ca^{2+}/CaM binding to our Thr^{286} phosphorylated CaMKII will be saturated (Kd is around 0.1 nM (58)) and binding of α-actinin to CaMKII inhibited (Fig. 6B). Indeed, we have previously shown that increasing α-actinin concentrations increasingly and eventually completely blocked CaMKII pull-down by GST-NR1 C0-C2'. Obviously under those conditions with Ca^{2+}/CaM present at concentrations equimolar to CaMKII and α-actinin bound to GST-NR1 C0-C2', CaMKII cannot bind to the α-actinin - NR1 C0 complex (cf. Fig. 7 in Ref. (7)). Hence, using the above strategy, we were able to observe an increase in CaMKII binding to GST-NR1 C0-C2' upon addition of extra CaM and the consequent displacement of α-actinin from GST-NR1 C0-C2'. The increase in

CaMKII binding is, therefore, due to the displacement of α-actinin by Ca^{2+}/CaM given that α-actinin can otherwise occlude CaMKII binding to GST-NR1 C0-C2'.

The biochemical studies presented here define interactions for different polypeptides and peptides in vitro. Details of these complex interactions could be altered in the native system with a fully assembled NMDA receptor complex, which provides additional interaction sites for CaMKII and α-actinin on its NR2 subunits. The observation that GST-NR1 C0-C2' cannot simultaneously bind α-actinin and CaMKII is quite different from the binding properties of densin-180. This postsynaptic protein also binds both CaMKII and α-actinin. In this case, however, densin-180 can simultaneously interact with CaMKII and α-actinin allowing the formation of ternary complexes (14,56).

Displacement of α-actinin from NR1 C0 by Ca^{2+}/CaM is thought to underlie Ca^{2+}-dependent desensitization of the NMDA receptor (28,29). This model raises the question whether CaMKII binding to NR1 C0 per se affects desensitization. In fact, ectopic co-expression of NR1 and NR2A with CaMKII in the non-neuronal HEK293 cell line leads to decreased desensitization as compared to NR1/NR2A only expression (59). These results would be consistent with the possibility that CaMKII binding to NR1 C0 reduces the desensitization that occurs when α-actinin is displaced by Ca^{2+}/CaM from NR1 C0 (28,29). Perhaps it is advantageous only in the presence of NMDA receptor-associated CaMKII to prevent desensitization of the NMDA receptor, thereby allowing for activation of an increased number of CaMKII subunits in the NR1-associated dodecameric CaMKII complexes. However, the interpretation of these data (59) is complicated by the observation that NR2A itself can to some degree bind CaMKII, albeit with lesser affinity (6,8,10,11). Furthermore, from these studies it is unclear whether the effect of CaMKII overexpression on NR1/NR2A channel activity is due to binding per se or due to a phosphorylation event by CaMKII.

Another unsolved question is whether binding to NR1 C0 is important for anchoring activated CaMKII at postsynaptic sites of activated synapses for more effective phosphorylation of neighboring postsynaptic substrates. It appears likely that NR1-associated CaMKII will require substantially less Ca^{2+} influx through the NMDA receptor for remaining activated as the Ca^{2+} concentration will be highest at the mouth of the NMDA receptor channel pore. Localization of CaMKII to the channel mouth would thereby promote re-autophosphorylation and counteracting the phosphatase activity that dephosphorylates CaMKII. Finally, given its unique dodecameric structure and its ability to reversibly self-associate (60,61), CaMKII may form a scaffold within the postsynaptic density involved in recruiting other synaptic proteins to postsynaptic sites (62,63). Support for such a model comes from a recent study that implicates both, CaMKII and F actin in activity-induced enlargement of postsynaptic spine heads (64). However, this study does not indicate whether CaMKII is involved as a structural component or by phosphorylating other proteins.

Displacement of α-actinin from NR1 C0 removes this link between the actin cytoskeleton and the NMDA receptor, thereby contributing to Ca^{2+}-dependent desensitization (28,29). The idea that α-actinin – F-actin connection may play a role in this desensitization is supported by earlier findings that disruption of F-actin also reduces NMDA receptor activity (27). A second potential role of this link is to localize NMDA receptors to postsynaptic sites as α-actinin and Factin are enriched in dendritic spines. If so, Ca^{2+}-induced dissociation of α-actinin from NR1 C0 could foster removal of the NMDA receptor from postsynaptic sites. Although there is evidence that a decrease in NMDA receptor activity results in increased postsynaptic accumulation of NMDA receptors the role of Ca^{2+} influx and potentially CaMKII in this process is unclear.

In conclusion, our work unravels critical details of the complex interplay between Ca^{2+}, CaM, CaMKII, and α-actinin for binding to the NMDA receptor NR1 C0 region. These details advance our understanding of molecular details that are important for postsynaptic signaling involved in synaptic plasticity and, likely, learning. These findings will be critical for guiding future functional studies.

ACKNOWLEDGMENT

The authors thank Drs. C. Otey, University of North Carolina, Chapel Hill, NC, and M. Sheng, Massachusetts Institute of Technology, Boston, MA, for providing the α-actinin-1 and -2 template constructs, respectively. We also thank Dr. D. D. Hall for the generation of the α-actinin-1 MBP expression construct and I. A. Evans, R. A. Newman and T. J. Witt for purifying the CaM used in these studies. Further, we appreciate the phosphospecific antibody against T305-phosphorylated CaMKII from Dr. A. Silva, University of California at Los Angeles, CA.

This work was supported by the NIH grant NS046450 (JWH) and GM057001 (MAS).

REFERENCES

1. Soderling TR, Chang B, Brickey D. Cellular signaling through multifunctional Ca2+/calmodulin-dependent protein kinase II. Journal of Biological Chemistry 2001;276:3719–3722. [PubMed: 11096120]
2. Malenka RC, Nicoll RA. Long-term potentiation-a decade of progress? Science 1999;285:1870–1874. [PubMed: 10489359]
3. Martin SJ, Grimwood PD, Morris RG. Synaptic plasticity and memory: an evaluation of the hypothesis. Annu Rev Neurosci 2000;23:649–711. [PubMed: 10845078]
4. Malenka RC, Bear MF. LTP and LTD: an embarrassment of riches. Neuron 2004;44:5–21. [PubMed: 15450156]
5. Collingridge GL, Isaac JT, Wang YT. Receptor trafficking and synaptic plasticity. Nat Rev Neurosci 2004;5:952–962. [PubMed: 15550950]
6. Leonard AS, Lim IA, Hemsworth DE, Horne MC, Hell JW. Calcium/calmodulin-dependent protein kinase II is associated with the N-methyl-D-aspartate receptor. Proc. Natl. Acad. Sci. USA 1999;96:3239–3244. [PubMed: 10077668]
7. Leonard AS, Bayer K-U, Merrill MA, Lim IA, Shea MA, Schulman H, Hell JW. Regulation of calcium/calmodulin-dependent protein kinase II docking to N-methyl-D-aspartate receptors by calcium/calmodulin and α-actinin. J. Biol. Chem 2002;277:48441–48448. [PubMed: 12379661]
8. Gardoni F, Schrama LH, van Dalen JJ, Gispen WH, Cattabeni F, Di Luca M. AlphaCaMKII binding to the C-terminal tail of NMDA receptor subunit NR2A and its modulation by autophosphorylation. FEBS Letters 1999;456:394–398. [PubMed: 10462051]
9. Gardoni F, Caputi A, Cimino M, Pastorino L, Cattabeni F, Di Luca M. Calcium/calmodulin-dependent protein kinase II is associated with NR2A/B subunits of NMDA receptor in postsynaptic densities. Journal of Neurochemistry 1998;71:1733–1741. [PubMed: 9751209]
10. Strack S, Colbran RJ. Autophosphorylation-dependent targeting of calcium/calmodulin-dependent protein kinase II by the NR2B subunit of the N-methyl-D-aspartate receptor. J. Biol. Chem 1998;273:20689–20692. [PubMed: 9694809]
11. Strack S, McNeill RB, Colbran RJ. Mechanism and regulation of calcium/calmodulin-dependent protein kinase II targeting to the NR2B subunit of the N-methyl-D-aspartate receptor. Journal of Biological Chemistry 2000;275:23798–23806. [PubMed: 10764765]
12. Bayer KU, De Koninck P, Leonard AS, Hell JW, Schulman H. Interaction with the NMDA receptor locks CaMKII in an active conformation. Nature 2001;411:801–805. [PubMed: 11459059]
13. Robison AJ, Bartlett RK, Bass MA, Colbran RJ. Differential Modulation of Ca2+/Calmodulin-dependent Protein Kinase II Activity by Regulated Interactions with N-Methyl-D-aspartate Receptor NR2B Subunits and {alpha}-Actinin. J Biol Chem 2005;280:39316–39323. [PubMed: 16172120]
14. Robison AJ, Bass MA, Jiao Y, Macmillan LB, Carmody LC, Bartlett RK, Colbran RJ. Multivalent Interactions of Calcium/Calmodulin-dependent Protein Kinase II with the Postsynaptic Density

Proteins NR2B, Densin-180, and {alpha}-Actinin-2. J Biol Chem 2005;280:35329–35336. [PubMed: 16120608]

15. Colbran RJ. Targeting of calcium/calmodulin-dependent protein kinase II. Biochem J 2004;378:1–16. [PubMed: 14653781]
16. Merrill MA, Chen Y, Strack S, Hell JW. Activity-driven postsynaptic translocation of CaMKII. Trends Pharmacol Sci 2005;26:645–653. [PubMed: 16253351]
17. Barria A, Muller D, Derkach V, Griffith LC, Soderling TR. Regulatory phosphorylation of AMPA-type glutamate receptors by CaM-KII during long-term potentiation. Science 1997;276:2042–2045. [PubMed: 9197267]
18. Lee HK, Barbarosie M, Kameyama K, Bear MF, Huganir RL. Regulation of distinct AMPA receptor phosphorylation sites during bidirectional synaptic plasticity. Nature 2000;405:955–959. [PubMed: 10879537]
19. Lee HK, Takamiya K, Han JS, Man H, Kim CH, Rumbaugh G, Yu S, Ding L, He C, Petralia RS, Wenthold RJ, Gallagher M, Huganir RL. Phosphorylation of the AMPA receptor GluR1 subunit is required for synaptic plasticity and retention of spatial memory. Cell 2003;112:631–643. [PubMed: 12628184]
20. Seeburg PH. The molecular biology of mammalian glutamate receptor channels. Trends Pharmacol. Sci 1993;14:297–303. [PubMed: 7504359]
21. Hollmann M, Heinemann S. Cloned glutamate receptors. Annual Review of Neuroscience 1994;17:31–108.
22. Sheng M, Cummings J, Roldan LA, Jan YN, Jan LY. Changing subunit composition of heteromeric NMDA receptors during development of rat cortex. Nature 1994;368:144–147. [PubMed: 8139656]
23. Blahos J II, Wenthold RJ. Relationship between N-methyl-D-aspartate receptor NR1 splice variants and NR2 subunits. Journal of Biological Chemistry 1996;271:15669–15674. [PubMed: 8663041]
24. Ehlers MD, Zhang S, Bernhardt JP, Huganir RL. Inactivation of NMDA receptors by direct interaction of calmodulin with the NR1 subunit. Cell 1996;84:745–755. [PubMed: 8625412]
25. Wyszynski M, Lin J, Rao A, Nigh E, Beggs AH, Craig AM, Sheng M. Competitive binding of α-actinin and calmodulin to the NMDA receptor. Nature 1997;385:439–442. [PubMed: 9009191]
26. Akyol Z, Bartos JA, Merrill MA, Faga LA, Jaren OR, Shea MA, Hell JW. Apo-calmodulin binds with its C-terminal domain to the N-methyl-D-aspartate receptor NR1 C0 region. J Biol Chem 2004;279:2166–2175. [PubMed: 14530275]
27. Rosenmund C, Westbrook GL. Calcium-induced actin depolymerization reduces NMDA channel activity. Neuron 1993;10:805–814. [PubMed: 7684233]
28. Zhang S, Ehlers MD, Bernhardt JP, Su CT, Huganir RL. Calmodulin mediates calcium-dependent inactivation of N-methyl-D-aspartate receptors. Neuron 1998;21:443–453. [PubMed: 9728925]
29. Krupp JJ, Vissel B, Thomas CG, Heinemann SF, Westbrook GL. Interactions of calmodulin and alpha-actinin with the NR1 subunit modulate Ca2+-dependent inactivation of NMDA receptors. J Neurosci 1999;19:1165–1178. [PubMed: 9952395]
30. Elgersma Y, Fedorov NB, Ikonen S, Choi ES, Elgersma M, Carvalho OM, Giese KP, Silva AJ. Inhibitory autophosphorylation of CaMKII controls PSD association, plasticity, and learning. Neuron 2002;36:493–505. [PubMed: 12408851]
31. Sorensen BR, Shea MA. Interactions between domains of apo calmodulin alter calcium binding and stability. Biochemistry 1998;37:4244–4253. [PubMed: 9521747]
32. Bradshaw JM, Hudmon A, Schulman H. Chemical quenched flow kinetic studies indicate an intraholoenzyme autophosphorylation mechanism for Ca2+/calmodulin-dependent protein kinase II. J Biol Chem 2002;277:20991–20998. [PubMed: 11925447]
33. Bhatt A, Kaverina I, Otey C, Huttenlocher A. Regulation of focal complex composition and disassembly by the calcium-dependent protease calpain. J Cell Sci 2002;115:3415–3425. [PubMed: 12154072]
34. Edlund M, Lotano MA, Otey CA. Dynamics of alpha-actinin in focal adhesions and stress fibers visualized with alpha-actinin-green fluorescent protein. Cell Motil Cytoskeleton 2001;48:190–200. [PubMed: 11223950]
35. Klee CB, Crouch TH, Krinks MH. Calcineurin: a calcium- and calmodulin-binding protein of the nervous system. Proc Natl Acad Sci U S A 1979;76:6270–6273. [PubMed: 293720]

36. Grab DJ, Berzins K, Cohen RS, Siekevitz P. Presence of calmodulin in postsynaptic densities isolated from canine cerebral cortex. J Biol Chem 1979;254:8690–8696. [PubMed: 468848]
37. Fabiato A, Fabiato F. Calculator programs for computing the composition of the solutions containing multiple metals and ligands used for experiments in skinned muscle cells. J Physiol (Paris) 1979;75:463–505. [PubMed: 533865]
38. Martell, A.; Sillen, L., editors. Stability Constants of Metal Ion Comples. Supplement No. 1. London: The Chemical Society; 1971.
39. Hashimoto Y, Schworer CM, Colbran RJ, Soderling TR. Autophosphorylation of Ca2+/calmodulin-dependent protein kinase II. Effects on total and Ca2+-independent activities and kinetic parameters. J Biol Chem 1987;262:8051–8055. [PubMed: 3110142]
40. Lou LL, Schulman H. Distinct autophosphorylation sites sequentially produce autonomy and inhibition of the multifunctional Ca2+/calmodulin-dependent protein kinase. J Neurosci 1989;9:2020–2032. [PubMed: 2542484]
41. Davare MA, Hell JW. Increased phosphorylation of the neuronal L-type Ca(2+) channel Ca(v)1.2 during aging. Proc Natl Acad Sci U S A 2003;100:16018–16023. [PubMed: 14665691]
42. Hall DD, Feekes JA, Arachchige Don AS, Shi M, Hamid J, Chen L, Strack S, Zamponi GW, Horne MC, Hell JW. Binding of protein phosphatase 2A to the L-type calcium channel Cav1.2 next to Ser1928, its main PKA site, is critical for Ser1928 dephosphorylation. Biochemistry 2006;45:3448–3459. [PubMed: 16519540]
43. Lakowicz, JR. Principles of Fluorescence Spectroscopy. 2d ed. New York: Kluwer Academic; 1999.
44. Beggs AH, Byers TJ, Knoll JH, Boyce FM, Bruns GA, Kunkel LM. Cloning and characterization of two human skeletal muscle alpha-actinin genes located on chromosomes 1 and 11. J Biol Chem 1992;267:9281–9288. [PubMed: 1339456]
45. Tang J, Taylor DW, Taylor KA. The three-dimensional structure of alpha-actinin obtained by cryoelectron microscopy suggests a model for Ca(2+)-dependent actin binding. J Mol Biol 2001;310:845–858. [PubMed: 11453692]
46. Walikonis RS, Jensen ON, Mann M, Provance DW Jr, Mercer JA, Kennedy MB. Identification of proteins in the postsynaptic density fraction by mass spectrometry. J Neurosci 2000;20:4069–4080. [PubMed: 10818142]
47. Peng J, Kim MJ, Cheng D, Duong DM, Gygi SP, Sheng M. Semiquantitative proteomic analysis of rat forebrain postsynaptic density fractions by mass spectrometry. J Biol Chem 2004;279:21003–21011. [PubMed: 15020595]
48. Meador WE, Means AR, Quiocho FA. Modulation of calmodulin plasticity in molecular recognition on the basis of x-ray structures. Science 1993;262:1718–1721. [PubMed: 8259515]
49. Strack S, Choi S, Lovinger DM, Colbran RJ. Translocation of autophosphorylated calcium/calmodulin-dependent protein kinase II to the postsynaptic density. J. Biol. Chem 1997;272:13467–13470. [PubMed: 9153188]
50. Shen K, Meyer T. Dynamic control of CaMKII Translocation in hippocampal neurons by NMDA receptor stimulation. Science 1999;284:162–166. [PubMed: 10102820]
51. Shen K, Teruel MN, Connor JH, Shenolikar S, Meyer T. Molecular memory by reversible translocation of calcium/calmodulin-dependent protein kinase II. Nature Neuroscience 2000;3:881–886.
52. Gleason MR, Higashijima S, Dallman J, Liu K, Mandel G, Fetcho JR. Translocation of CaM kinase II to synaptic sites in vivo. Nat Neurosci 2003;6:217–218. [PubMed: 12563265]
53. Otmakhov N, Tao-Cheng JH, Carpenter S, Asrican B, Dosemeci A, Reese TS, Lisman J. Persistent accumulation of calcium/calmodulin-dependent protein kinase II in dendritic spines after induction of NMDA receptor-dependent chemical long-term potentiation. J Neurosci 2004;24:9324–9331. [PubMed: 15496668]
54. Gu Z, Jiang Q, Yuen EY, Yan Z. Activation of Dopamine D4 Receptors Induces Synaptic Translocation of Ca2+/Calmodulin-Dependent Protein Kinase II in Cultured Prefrontal Cortical Neurons. Mol Pharmacol 2006;69:813–822. [PubMed: 16365279]
55. Strack S, Robison AJ, Bass MA, Colbran RJ. Association of calcium/calmodulin-dependent kinase II with developmentally regulated splice variants of the postsynaptic density protein densin-180. Journal of Biological Chemistry 2000;275:25061–25064. [PubMed: 10827168]

56. Walikonis RS, Oguni A, Khorosheva EM, Jeng CJ, Asuncion FJ, Kennedy MB. Densin-180 forms a ternary complex with the (alpha)-subunit of Ca2+/calmodulin-dependent protein kinase II and (alpha)-actinin. J Neurosci 2001;21:423–433. [PubMed: 11160423]
57. Dhavan R, Greer PL, Morabito MA, Orlando LR, Tsai LH. The cyclin-dependent kinase 5 activators p35 and p39 interact with the alpha-subunit of Ca2+/calmodulin-dependent protein kinase II and alpha-actinin-1 in a calcium-dependent manner. J Neurosci 2002;22:7879–7891. [PubMed: 12223541]
58. Hudmon A, Schulman H. Neuronal CA2+/calmodulin-dependent protein kinase II: the role of structure and autoregulation in cellular function. Annu Rev Biochem 2002;71:473–510. [PubMed: 12045104]
59. Sessoms-Sikes S, Honse Y, Lovinger DM, Colbran RJ. CaMKIIalpha enhances the desensitization of NR2B-containing NMDA receptors by an autophosphorylation-dependent mechanism. Mol Cell Neurosci 2005;29:139–147. [PubMed: 15866054]
60. Hudmon A, Schulman H. Structure-function of the multifunctional Ca2+/calmodulin-dependent protein kinase II. Biochem J 2002;364:593–611. [PubMed: 11931644]
61. Hudmon A, Lebel E, Roy H, Sik A, Schulman H, Waxham MN, De Koninck P. A mechanism for Ca2+/calmodulin-dependent protein kinase II clustering at synaptic and nonsynaptic sites based on self-association. J Neurosci 2005;25:6971–6983. [PubMed: 16049173]
62. Lisman JE, Zhabotinsky AM. A model of synaptic memory: a CaMKII/PP1 switch that potentiates transmission by organizing an AMPA receptor anchoring assembly. Neuron 2001;31:191–201. [PubMed: 11502252]
63. Lisman J, Schulman H, Cline H. The molecular basis ofCaMKII function in synaptic and behavioral memory. Nature Neurosci 2002;3:175–190.
64. Matsuzaki M, Honkura N, Ellis-Davies GC, Kasai H. Structural basis of long-term potentiation in single dendritic spines. Nature 2004;429:761–766. [PubMed: 15190253]

Abbreviations used are

AMPA, α-amino-3-hydroxy-5-methyl-4-isoxazole proprionic acid
CaMKII, Ca^{2+}/calmodulin-dependent kinase II
CaM, calmodulin
eq, molar equivalents
GST, glutathione *S*-transferase
LTP, long term potentiation
MBP, maltose binding protein
NMDA, *N*-methyl-D-aspartate
NR1C0p, NMDA receptor NR1 subunit C-terminal peptide consisting of residues 838–865
NTA, nitrilotriacetic acid
PCR, polymerase chain reaction
PVDF, polyvinylidene diflouride
SDS, sodium dodecylphosphate
SDS-PAGE, SDS-polyacrylamide gel electrophoresis

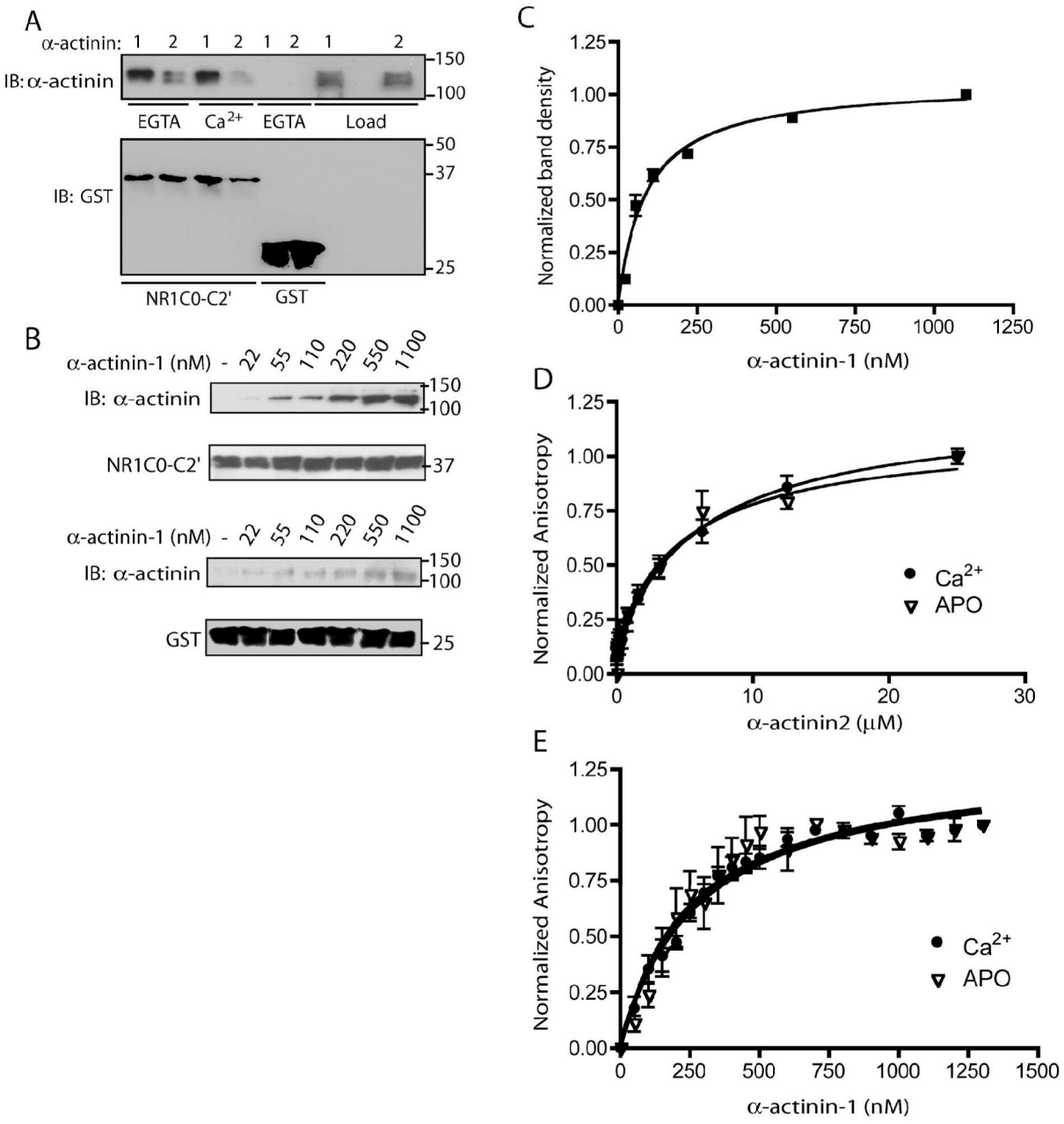

Figure 1. α-Actinin-1 binds NR1 C0-C2′ with higher affinity than α-actinin-2

Glutathione Sepharose was loaded with GST-NR1 C0-C2′ or GST alone (the nominal concentration for GST-NR1 C0-C2′ was about 12.5 nM for the 50 μl incubation volumes). ***A***, Incubation with 4 μM MBP-α-actinin-1 or -2 in the presence of either EGTA (lanes 1,2,5,6) or Ca^{2+}(lanes 3,4). The upper portion of each blot was probed with anti-MBP to detect MBP-tagged α-actinin (top panel) and the lower portion with anti-GST to demonstrate comparable amounts of NR1 C0-C2′ and GST were present in each sample (lower panel; in this experiment GST was in excess over GST-NR1 C0-C2′, increasing the stringency for testing non-specific binding). Five percent of the amount of MBP-α-actinin-1 and -2 used for each pull-down was applied directly to SDS-PAGE to confirm that similar amounts of the two isoforms were added to the immobilized fusion proteins (***A***, lanes 7 and 8). While α-actinin-1 and -2 both specifically

bind to GST-NR1 C0-C2′, α-actinin-1 shows more robust binding under both EGTA and Ca^{2+} conditions (***A***, compare lanes 1 and 3 with 2 and 4). Similar results were obtained in several other experiments. ***B***, increasing amounts of MBP-α-actinin-1 were incubated with NR1 C0-C2′ GST (top two panels) and GST (bottom two panels; nominal concentration of both GST proteins was about 12.5 nM). Blots were probed with anti-MBP to detect MBP-tagged α-actinin (first and third panels) and anti-GST to demonstrate comparable amounts of GST-NR1 C0-C2′ and GST were used (second and fourth panels). Immunosignals for α-actinin-1 were quantified with Adobe Photoshop. Signals from non-specific α-actinin-1 binding to GST alone were subtracted before the data were graphed in GraphPad Prism (4.0a). ***C***, graphed data from **B** show that α-actinin-1 binding was saturable with a kD of ~ 87 nM. ***D, E***, fluorescence anisotropy of the fluorescein-labeled peptide NR1C0p was monitored (λ_{ex} of 496 nm; λ_{em} of 520 nm) as a function of increasing amounts of His-tagged α-actinin-2 and MBP-tagged α-actinin-1 under Ca^{2+}-depleted and -saturated conditions. Nonlinear analysis of the titration curve of NR1C0p indicated an apparent Kd value of 2.75 μM for α-actinin-2 under both conditions, 239 versus 237 nM for α-actinin-1 under Ca^{2+}-depleted and -saturated conditions. Each titration curve in C, D, and E was from 3–6 independent experiments.

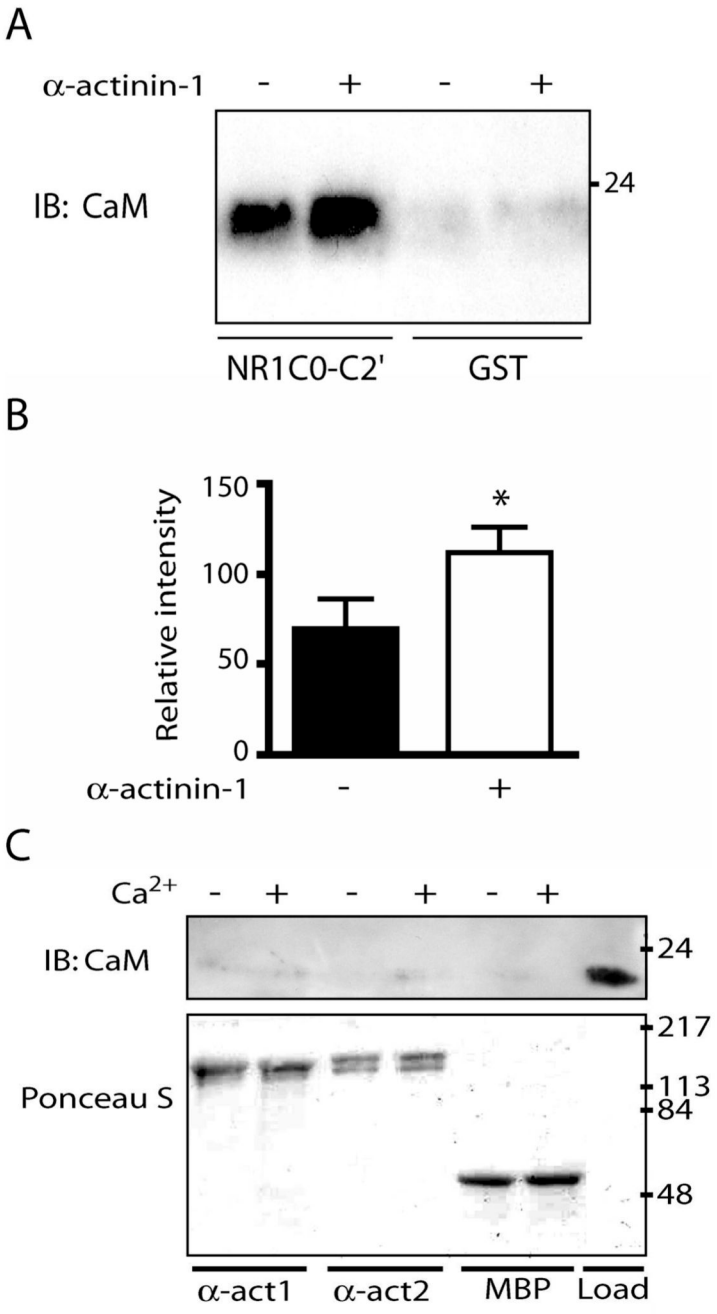

Figure 2. Apo-CaM and α-actinin simultaneously bind to NR1 C0-C2′ GST under Ca^{2+}-depleted conditions

A, GST-NR1 C0-C2′ or GST (~5 nM nominal concentration for the 50 μl sample volumes during CaM binding) were immobilized on glutathione Sepharose, washed, incubated with 2.5 μM CaM ± 6 μM α-actinin-1, quickly washed twice and analyzed by immunoblotting with anti-CaM. Blots were stained with Ponceau S before probing to confirm that similar amounts of GST and GST fusion protein were present (not illustrated). Similar results were obtained when either 1 μM CaM ± 6 μM α-actinin-1 or 4 μM CaM ± 4 μM α-actinin were added to 5 and 12.5 nM NR1 C0-C2′, respectively (data not illustrated). ***B***, immunosignals for CaM from several experiments were quantified with Adobe Photoshop (shown as mean ± SD; *n*=4).

Signals from CaM binding to GST (e.g., right two lanes in **A**) were subtracted before the data were graphed in GraphPad Prism (4.0a). There was a statistically significant increase in the amount of CaM binding in the presence of α-actinin (as determined by paired t-test). ***C***, α-actinin and CaM do not directly bind. MBP-tagged α-actinin-1, -2 and MBP alone were immobilized on amylose resin, incubated with 50 μM CaM in HEPES buffer ± 10 mM $CaCl_2$, washed as samples in **A**, and analyzed by immunoblotting with anti-CaM. Approximately 1.5% of the CaM used in the binding assay was loaded directly on the gel in the lane at the very right. This signal provides a positive control for the anti-CaM blotting and a measure of how much maximal signal could be expected if all CaM would have bound (multiply band intensity with 66.6). Blots were stained with Ponceau S (lower panel) before probing to confirm that similar amounts of fusion protein were present. Similar results were obtained in several other experiments.

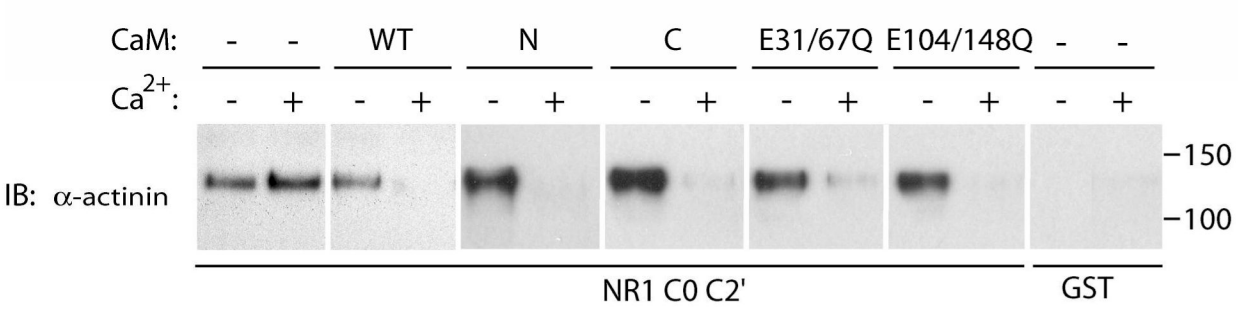

Figure 3. The N- and the C-domain of CaM compete with α-actinin for binding to NR1 C0-C2′ under Ca^{2+} conditions

Approximately 5 nM GST-NR1 C0-C2′ or equal amount of GST were immobilized on glutathione Sepharose and incubated in the absence or presence of 10 mM Ca^{2+} with 200 nM MBP-tagged α-actinin-1 and 10 μM of one of the following: full-length CaM ($CaM_{1–148}$); N domain of CaM ($CaM_{1–80}$); C domain of CaM ($CaM_{76–148}$); full-length E31/67Q mutant CaM, which does not bind Ca^{2+} in its N-domain; full-length E104/148Q mutant CaM, which does not bind Ca^{2+} in its C-domain. Blots were probed with anti-MBP. In the absence of CaM, Ca^{2+} does not affect α-actinin binding to NR1 C0-C2′ (panel on very left). GST was used to demonstrate the absence of non-specific binding of MBP-α-actinin-1 to GST (panel on very right). Before probing blots were stained with Ponceau S to confirm that similar amounts of GST fusion protein were present (not shown). Full-length CaM, N-domain, C-domain and both full-length CaM mutants antagonized α-actinin binding in a Ca^{2+}-dependent manner. Comparable results were obtained in multiple other experiments.

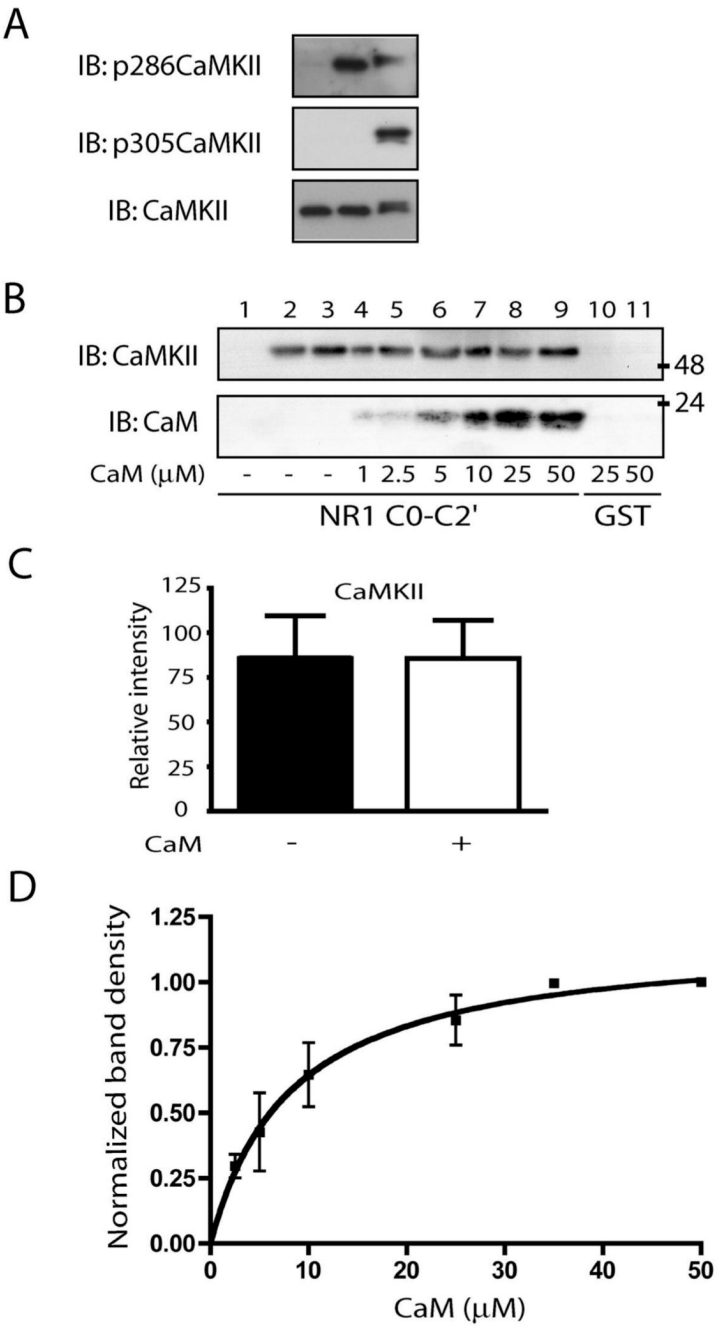

Figure 4. CaMKII and CaM simultaneously bind to NR1 C0-C2′

A, CaMKII is differentially phosphorylated under various conditions in vitro. CaMKII was incubated either with Ca^{2+}-CaM only (no autophosphorylation; left lane), Ca^{2+}-CaM plus Mg-ATP on ice for 30 sec (selective T286 autophosphorylation; middle lane), or Ca^{2+}-CaM plus Mg-ATP on ice for 30, followed by an additional incubation at 30°C for 10 minutes with EGTA (T286 plus T305 autophosphorylation; right lane). Samples were analyzed by immunoblotting with the general antibody against CaMKIIα (bottom), the phosphospecific antibody against T286 (top) and the phosphospecific antibody against T305 (middle). ***B***, GST or GST-NR1 C0-C2′ GST (11.4 nM) were immobilized on glutathione Sepharose and incubated with excess CaMKII (0.55 μg; pre-autophosphorylated on T286 with Mg-ATP and CaM as required for

NR1 C0 binding; the nominal concentration of the CaM-CaMKII complex assuming monomeric CaMKII from the phosphorylation reaction in the 50 µl binding volume was 200 nM). Excess of CaM-CaMKII that was not bound to the resin was washed away before extensive incubations with increasing amounts of CaM and a final washing step. Blots were probed with anti-CaMKII (top panel) and anti-CaM antibodies (lower panel). Before probing blots were stained with Ponceau S to confirm that similar amounts of GST fusion protein were present (not shown). As expected, unphosphorylated CaMKII (ATP was omitted from the phosphorylation mixture) did not bind (lane 1). Lanes 2 and 3 are duplicate samples when no CaM, except that required to activate CaMKII during the phosphorylation reaction, was added during the final incubation. Lanes 4–9 show samples with increasing amounts of CaM added to the CaMKII/NR1 C0-C2′ fusion protein complex as indicated. ***C***, there was no statistically significant difference in the binding of CaMKII to GST-NR1 C0-C2′ GST with and without 50 µM CaM (as examined by paired t-test). Immunosignals for CaMKII and CaM were quantified with Adobe Photoshop. Shown are means of 4 independent experiments (see B; error bars ± SEM). ***D***, data for increasing amounts of CaM (see B) were graphed and a monoexponential saturation curve fitted in GraphPad Prism (4.0a). CaM binding was saturable with an apparent kD of ~ 8 µM in this assay.

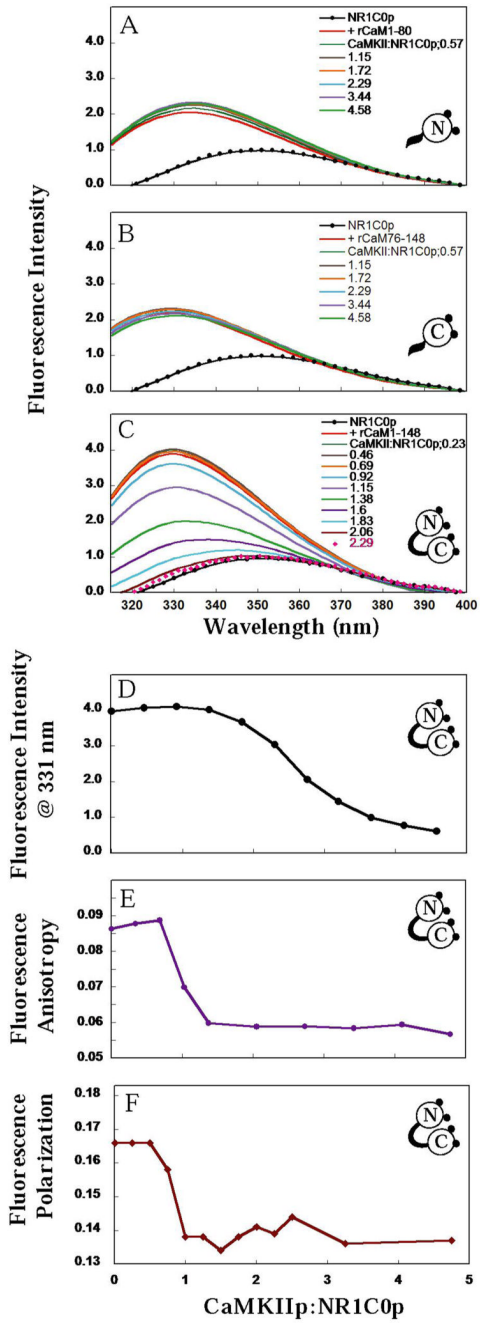

Figure 5. Competition between NR1C0p and CaMKIIp for CaM

Changes in the emission properties of NR1C0p in complex with (***A***) $CaM_{1–80}$, (***B***) $CaM_{76–148}$, and (***C***) $CaM_{1–148}$ upon addition of increasing CaMKIIp in the presence of Ca^{2+}. NR1C0p alone is represented by the solid black line with closed circles. Addition of $CaM_{1–80}$, $CaM_{76–148}$, and $CaM_{1–148}$ causes a left-shift of the emission spectrum (solid red lines represent the initial NR1C0p/CaM complexes). Spectra of the mixture after increasing additions of CaMKIIp peptide are shown as colored lines as indicated in the right portion of each panel. For full-length CaM, the spectrum representing the last addition of CaMKIIp (at a ratio of 2.29 CaMKIIp:NR1C0p) approaches the original spectrum and is indicated by closed red circles. The decrease in the fluorescence intensity of full NR1C0p-$CaM_{1–148}$ complex at

331 nm (see C) is plotted *vs.* CaMKIIp:NR1C0p ratio in (***D***). Fluorescence anisotropy measured for the intrinsic Trp^{21} fluorescence of NR1C0p (***E***) and fluorescent polarization of the fluorescein of the fluorescein-labeled NR1C0p (***F***) is plotted against the CaMKIIp:NR1C0p ratio. All measurements indicate that binding of full length CaM to CaMKIIp releases the NR1C0p as the curves shift back towards the original characteristics of the NR1C0p in the absence of CaM. Isolated N- or C-domain only bind NR1C0p but not CaMKIIp, i.e., there is no back shifting of the NR1C0P-CaM curves as expected (***A, B***).

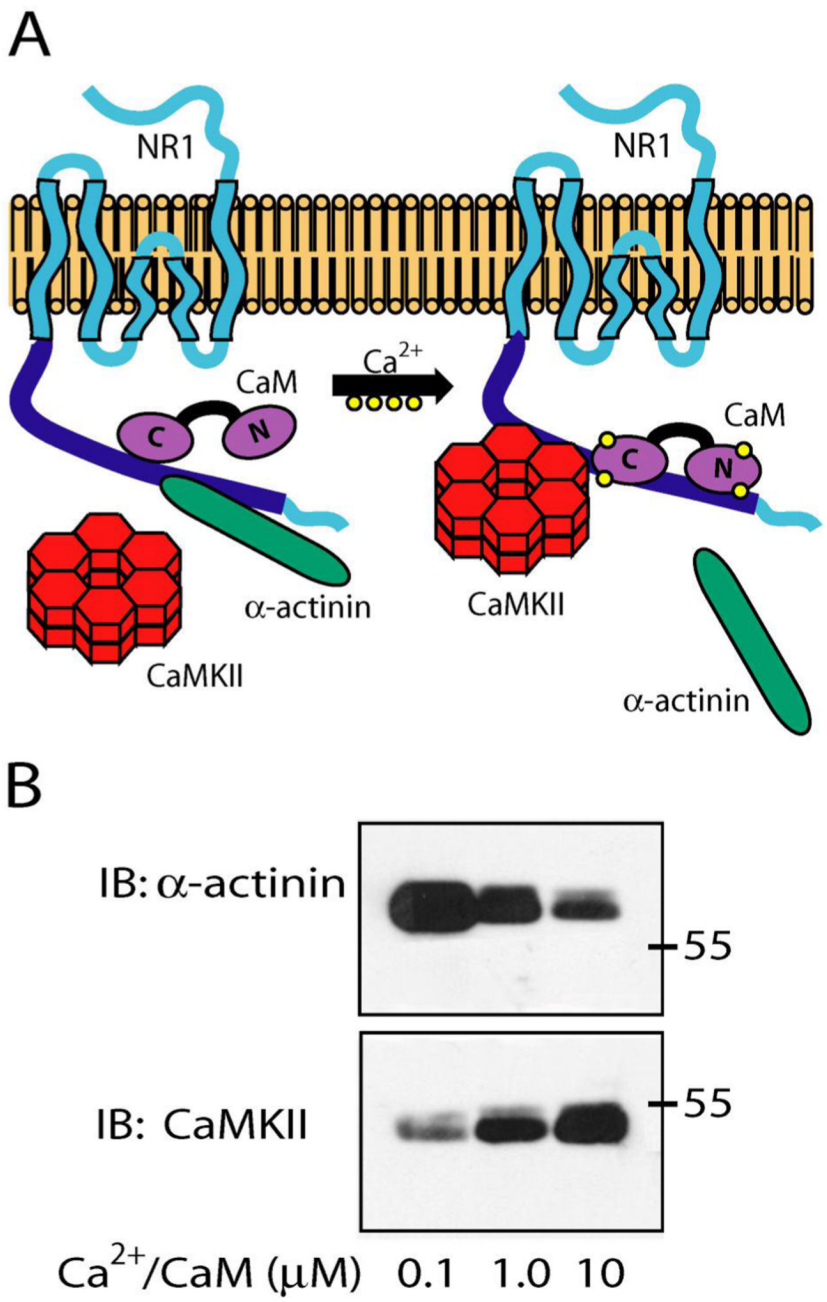

Figure 6. Ca^{2+}-CaM promotes CaMKII binding to NR1 C0-C2′ by displacing α-actinin

A, schematic representation of the proposed interactions between CaMKII, α-actinin, and CaM with the NR1 subunit of the NMDA receptor under apo and Ca^{2+}-conditions. Under Ca^{2+}-free (apo) conditions, α-actinin and the C-domain of CaM are bound to the C0 region of the NR1 subunit. α-Actinin competes with CaMKII for binding to NR1 C0. Upon activation of the NMDA receptor and the subsequent Ca^{2+} influx, the C-domain of Ca^{2+}-CaM rearranges relative to NR1 C0 and the N-domain now directly binds NR1 C0. Through these changes, CaM antagonizes α-actinin binding to the C0 region via both its N- and C-domains. The removal of α-actinin by Ca^{2+}-CaM promotes binding of activated CaMKII to NR1 C0 resulting in the simultaneous binding of Ca^{2+}-CaM and CaMKII to NR1 C0 via different sites of the

putative C0 α-helix. ***B***, to test the proposed model, GST and GST-NR1 C0-C2′ (90 nM) were immobilized on glutathione Sepharose and incubated with 1 μM T7-tagged α-actinin fusion protein for 2 hours to reach equilibrium. 0.1 μM of autophosphorylated CaMKII and 0.1, 1.0, or 10 μM CaM were added to the incubation mixture in the presence of 500 μM $CaCl_2$ for an additional 2 hours. Blots were probed with anti-CaMKII, stripped and reprobed with anti-T7 to detect the α-actinin fusion protein. The addition of increasing amounts of Ca^{2+}-CaM decreased the amount of α-actinin binding while increasing the amount of CaMKII binding to GST-NR1 C0-C2′.